Enzymatic Synthesis of Furan-Based Copolymers: Material Characterization and Potential for Biomedical Applications

Martyna Sokołowska[1], Moein Zarei[1], Miroslawa El Fray[1*]

[1]West Pomeranian University of Technology, Szczecin, Faculty of Chemical Technology and Engineering, Department of Polymer and Biomaterials Science, Al. Piastow 45, 71-311 Szczecin, Poland

*Corresponding author: mirfray@zut.edu.pl

Abstract

Background: Today's growing demand for advanced and sustainable polyester materials is driven by an increasing awareness of the environmental impact of traditional materials, emphasizing the need for eco-friendly alternatives. Sustainability has become central in materials development, including the biomedical field, where biobased and environmentally friendly solutions are rapidly growing field.

Objectives: This research aims to comprehensively evaluate a new enzymatically catalyzed furan-based copolymer, poly(decamethylene furanoate)-co-(dilinoleic furanoate) (PDF-DLF), with a 70-30 wt% hard-to-soft segment ratio. The study explores its performance across medical applications, with a particular focus on its potential as nanofibrous scaffolding materials.

Materials and Methods: PDF-DLF was synthesized from biobased monomers using *Candida antarctica* lipase B (CAL-B) as the biocatalyst. Material characterization included dynamic mechanical thermal analysis (DMTA) to assess their mechanical behavior and thermal properties. Enzymatic degradation studies determined biodegradability while cytotoxicity tests established *in vitro* biocompatibility. The copolymer was electrospun into nanofibers, with SEM analyzing their morphology.

Results: PDF-DLF displays mechanical and thermal properties indicating high storage modulus and two main temperature transitions. Enzymatic degradation studies and cytotoxicity assessments confirm biodegradability and *in vitro* biocompatibility. Successful electrospinning transforms the copolymer into nanofibers with diameters ranging from 500 to 700 nm.

https://doi.org/10.26434/chemrxiv-2023-0095d-v2 **ORCID:** https://orcid.org/0000-0002-2474-3517 Content not peer-reviewed by ChemRxiv. **License:** CC BY 4.0

Conclusions: This study significantly advances sustainable polyesters with versatile processing capabilities. The successful electrospinning highlights its potential as a biodegradable scaffold for medical engineering, supported by biocompatibility and sufficient mechanical properties. It opens new opportunities for sustainable materials in critical biomedical industries, including tissue engineering.

Keywords: 2,5-furandicarboxylate, enzymatic synthesis, bio-based monomers, CAL-B, block copolymers.

1. Introduction

In the ever-evolving field of biomedical engineering, the quest for sustainable materials that are both environmentally friendly and functionally versatile has never been more imperative. Traditional polymers often rely on petroleum-derived compounds, which not only contribute to environmental pollution but also raise concerns regarding their biocompatibility in biomedical applications [1,2].

In this context, 2,5-furandicarboxylic acid (FDCA) emerges as a promising candidate with its unique potential derived from natural resources, offering an alternative to petrochemical monomers [3,4]. FDCA is a carbohydrate compound within the furfural group, derived from polysaccharides, starch, or lignocellulose. Its chemical structure bears resemblance to terephthalic acid (TPA), the primary petrochemical monomer for the synthesis of semicrystalline aromatic polyesters like poly(ethylene terephthalate) (PET) or poly(butylene terephthalate) (PBT) [5–8]. Notably, numerous publications have demonstrated FDCA's capacity to yield materials with superior properties and enhanced polymer chain orientation compared to their TPA analogs, which impart significant advantages [9–12]. Such attributes are particularly critical in tissue engineering, where the mechanical properties of the material must often align with the specific tissue being replaced or repaired.

Interestingly enough, the versatility of copolymers containing both hard and soft segments, as seen in the material under investigation, offers the advantage of tailoring the final properties to meet the precise requirements of different tissue engineering applications [13].

A growing interest in the conversion and utilization of biomass, coupled with rapid developments in the biorefinery industry, has introduced a wide spectrum of opportunities in the production of novel monomers and polymers from renewable sources [14–19]. However, questions persist about the selection of the best and most selective catalyst. Conventionally, PET material is produced in melt processes using antimony-based catalysts in the form of oxide or acetate, known for their high

https://doi.org/10.26434/chemrxiv-2023-0095d-v2 **ORCID:** https://orcid.org/0000-0002-2474-3517 Content not peer-reviewed by ChemRxiv. **License:** CC BY 4.0

performance and ability to withstand elevated temperatures. Nevertheless, a significant drawback arises from the presence of residual metals within the polymeric material, which is challenging to remove due to strong metal-ester interactions. This can lead to material discoloration and raise environmental concerns upon disposal, potentially disqualifying the polymer's use in various applications, including the medical industry [16,20].

To address this issue, in this work, we used enzymes that have emerged as a compelling alternative catalyst derived from natural resources. Among enzymes, *Candida antarctica* lipase B (CAL-B) stands out due to its stability and high reactivity, with its unique structure enabling high regio-, enantio-, stereoselectivity, and the ability to function under mild reaction conditions [21–24]. As confirmed in previous studies, enzymatic catalysis results in a more regular structure in copolyesters compared to metal-catalyzed processes [25,26]. This feature opens up opportunities to obtain optically pure materials with well-defined chemical structures, particularly valuable in the pharmaceutical industry. CAL-B-induced polymerization has already been successfully applied to various polymer types, including polyesters based on 2,5-bis(hydroxymethyl)furan, vegetable oils, sugars, and 3,6-dianhydrohexitol [17,27–30]. By using monomers and catalyst originating from biomass resources it is possible to provide sustainable and safe material for biomedical applications.

Advances in the tissue engineering field have brought much attention in terms of scaffold fabrication, such as with biodegradable polyester nanofibers. The justification for using nanofibers for tissue engineering is that the nonwoven polymeric meshwork is a close representation of the nanoscale protein fiber meshwork in the native extracellular matrix (ECM) [31]. The electrospinning technique is a promising way to fabricate a controllable continuous nanofiber scaffold mimicking the ECM structure. Electrospun nanofibers provide a high surface-to-volume ratio and high porosity as a promising scaffold for tissue engineering. Because the degradation behaviors of scaffolds significantly affect new tissue regeneration, the degradation of the material becomes one of the crucial factors when considering using polyester nanofibers as scaffolds in tissue engineering.

Given the above information, in this research, we are focusing on a comprehensive exploration of furan-based copolymers, investigating their potential as scaffolds in the dynamic field of biomedical engineering, emphasizing their ecological advantages and the integration of enzymatic catalysis for improved sustainability. Our focus extends to the electrospinning technique applied to poly(decamethylene furanoate-dilinoleic furanoate) (PDF-DLF) with 70 wt% PDF segments, introducing a groundbreaking avenue for the creation of sustainable biomaterials. This innovative approach aims to

https://doi.org/10.26434/chemrxiv-2023-0095d-v2 **ORCID:** https://orcid.org/0000-0002-2474-3517 Content not peer-reviewed by ChemRxiv. **License:** CC BY 4.0

not only assess the biocompatibility and biodegradation profile of the manufactured material but also to evaluate its suitability for processing into nanofibers.

Experimental

1.1 Materials

The following chemicals were purchased from Sigma-Aldrich (Poznan, Poland): diphenyl ether (DE; ≥99%), mouse fibroblasts L929 EACC, Dulbecco's Modified Eagle's Medium (DMEM), Dulbecco's Phosphate Buffered Saline (DPBS), resazurin, penicillin, streptomycin, bovine fetal serum (FBS), L-glutamine. Polycaprolactone CAPA 6430 was purchased from Perstop (Warrington, UK). 1,10-decanediol (DDO; ≥99%) was acquired from Acros Organics (Geel, Belgium). Dimethyl 2,5-furandicarboxylate (DMFDCA; ≥99%) was obtained from Fluorochem (Lodz, Poland). Dilinoleic diol (DLD; ≥96.5%) (trade name: Pripol™ 2033) was obtained from Cargill Bioindustrials (Gouda, The Netherlands). Chloroform (≥98.5%) was purchased from Chempur (Piekary Slaskie, Poland) and methanol (≥99.8%) was acquired from Stanlab (Lublin, Poland). *Candida antarctica* lipase B (CAL-B) covalently immobilized on polyacrylate beads (300-500 μm; ≥95%, Fermase CALB™ 10000), with a nominal activity of 10 000 PLU/g (propyl laurate units per gram dry weight) was purchased from Fermenta Biotech Ltd, Mumbai and Enzyme Catalyzed Polymers LLC (Akron, OH, USA). Before use, CAL-B was pre-dried under vacuum for 24h at 40 °C, and diphenyl ether was stored over 4Å molecular sieves. The rest of the chemicals were used as received.

1.2 CAL-B catalyzed polycondensation

To produce poly(decamethylene furanoate)-co-(dilinoleic furanoate) (PDF-DLF) copolyester with a 70-30 wt.% hard to soft segment ratio, a two-step polycondensation reaction was carried out in diphenyl ether at different temperatures, following the protocol outlined in our prior study [32].

1.3 Dynamic mechanical thermal analysis

To determine the storage and loss modulus, a PDF-DLF sample for dynamic mechanical thermal analysis (DMTA) was fabricated by melt-pressing within a temperature of 110 °C. The specimen had dimensions of 100 μm in thickness, 1 mm in width, and 50 mm in length. The measurements were carried out in tensile mode using the DMA Q800 apparatus from TA Instruments. The analysis was conducted at a constant frequency of 1 Hz, a heating rate of 2 °C/min, and an amplitude of 60.

https://doi.org/10.26434/chemrxiv-2023-0095d-v2 **ORCID:** https://orcid.org/0000-0002-2474-3517 Content not peer-reviewed by ChemRxiv. **License:** CC BY 4.0

1.4 Enzymatic degradation

Enzymatic degradation studies were conducted on melt pressed films (prepared according the same protocol as for DMTA studies) using lipase produced by *Pseudomonas cepacia* bacteria. The enzyme was prepared in Dulbecco's PBS sterile phosphate buffer with a concentration of 25 U/ml and a pH of 7.25. To prevent the bacteria from multiplying, 0.02% sodium azide was added. Degradation was carried out at a temperature of 37°C for 35 days, and measuring points were scheduled every 7 days. The degradation medium was replaced every 48 hours to maintain enzyme activity. Each measuring point consisted of 4 samples, which were subjected to weight, microscopic, and SEC analysis. Enzymatic degradation was performed on discs of the test material, which were 6 mm in diameter and 100 μm in thickness. To ensure sterile conditions during the enzymatic degradation tests, all operations were performed under a laminar chamber. The discs of both the test material and reference material were sterilized with UVC radiation for 30 minutes on each side.

To monitor enzymatic degradation progress, the samples underwent analysis for mass loss, molecular weight, morphological, and structural changes. Mass loss was quantified using equation (1), where m_0 is sample mass before degradation and m_d is a mass of vacuum-dried sample (37 °C, -60 kPa, 48 h) after degradation. Molecular weight analysis was performed via Size Exclusion Chromatography (SEC) using a Thermofisher (HLC-8320) system equipped with four detection systems: a dual absorbance UV (UV, Waters 2487, wavelength λ = 254-280 nm), multi-angle laser light scattering (MALLS, Wyatt DAWN), a refractive index detector (RI, Wyatt Optilab®), and a viscometer (VIS, Wyatt ViscoStar®) detectors. The determination of average molar (apparent) mass (M_n, M_w) and dispersity ($Đ$, M_w/M_n) was carried out through gel chromatography. The mobile phase used was $CHCl_3$ (HPLC grade, Alfa Aesar) at a flow rate of 1 mL/min, with a sample concentration of 15 mg/mL and an injected volume of 50 μL. Before injection onto the column, the sample solutions underwent filtration using a 0.20 μm SRP 20 filter. Absolute molecular masses were derived by processing the data with ASTRA version 8.1.2 software, assuming 100% recovery from the columns.

Structural alterations were evaluated through Attenuated Total Reflection–Fourier Transform Infrared (ATR–FTIR) spectra, recorded on a Bruker ALPHA spectrometer within the spectral range of 400 to 4000 cm^{-1}, employing a resolution of 2 cm^{-1}. Notably, 32 scans were conducted for each sample. Morphological changes were examined utilizing a scanning electron microscope (SEM) equipped with ultra-high resolution (UHR), specifically on a Hitachi SU8020 apparatus.

https://doi.org/10.26434/chemrxiv-2023-0095d-v2 **ORCID:** https://orcid.org/0000-0002-2474-3517 Content not peer-reviewed by ChemRxiv. **License:** CC BY 4.0

$$Mass\ loss = \frac{m_0 - m_d}{m_0} \cdot 100\% \qquad (1)$$

1.5 Cytotoxicity assessment

The cytotoxic potential and growth-inhibitory effects of the PDF-DLF copolyester were assessed in cell culture using L929 mouse fibroblasts, following ISO 1993-5 guidelines. L929 cells (passages 9-11) were cultured in growth media consisting of DMEM, 10% FBS, 2 mM L-glutamine, 100 U/ml penicillin, and 100 µg/ml streptomycin in T25 flasks. For the experiments, sub-confluent T25 flask cultures of L929 cells were trypsinized, and 1×10^4 cells were seeded per well in a 96-well plate. Simultaneously, 100 µm-thick films of PBF-DLF copolyester and a reference material (polycaprolactone PCL CAPA® 6430) were cut into three 6 cm^2 samples, which were then sterilized under UV-C light for 15 minutes on each side. Subsequently, the material samples (n=3) were sectioned into smaller pieces and placed in a 24-well plate, with 1 ml of medium added to each well. The plates were incubated for 24 hours at 37 °C in a 5% CO_2 environment to allow the cells to adhere and spread. After this incubation, the media were aspirated, and 100 µl of growth media containing extracts from the tested materials were added to the wells (with 6 technical replicates performed for each material). A sham control was prepared by adding 100 µl of pure growth media. The plate was incubated for an additional 24 hours, after which cell viability was evaluated using an inverted light microscope (Delta Optical IB-100) and a resazurin viability assay [23]. The assay was conducted with a fluorescent plate reader (Biotek Synergy HTX) at an excitation wavelength of 540 nm and an emission wavelength of 590 nm. During the resazurin viability assay, complete growth media were added to an empty well without cells, serving as the blank. The results obtained were expressed as the percentage of normalized cell viability (CV%), calculated using Equation (2) [33]:

$$CV\% = \frac{(FL_s - FL_b)}{(FL_c - FL_b)} \times 100\% \quad (2)$$

where FL is the fluorescence intensity and indexes *s*, *b*, and *c* refer to sample, blank, and control, respectively.

1.6 Electrospinning

In the pursuit of optimizing the electrospinning process for the synthesis of our novel polymer, a systematic exploration of key parameters was conducted. The home-made electrospinning setup employed in this study comprised a syringe pump, a high voltage power supply, and a collector. Various parameters, namely needle diameter,

https://doi.org/10.26434/chemrxiv-2023-0095d-v2 **ORCID:** https://orcid.org/0000-0002-2474-3517 Content not peer-reviewed by ChemRxiv. **License:** CC BY 4.0

applied voltage, flow rate, distance between the needle tip and the collector, and polymer solution concentration, were subjected to meticulous optimization. The distance between the needle tip and the collector varied at 10 cm, 15 cm, and 20 cm, while the applied voltage ranged from 10 kV to 20 kV. Simultaneously, the flow rate of the polymer solution was adjusted at 2 mL/h, 5 mL/h, and 10 mL/h. A high-purity solvent, chloroform, was utilized for the polymer solution, and concentrations spanning 1% to 50% were explored, with observations facilitated by a light microscope Delta Optical Evolution 300. Morphology of resulting fibers was examined using a scanning electron microscope (SEM) on a Hitachi SU8020 apparatus with ultra-high resolution (UHR).

2 Results and discussion

Fully biobased PDF-DLF copolymer containing 70 wt% poly(decamethylene furanoate) (PDF) as the hard segments and 30 wt% poly(dilinoleic furanoate) (DLF) as the soft segments was successfully synthesized *via* temperature-varied two-step method in diphenyl ether using CAL-B as biocatalyst according to the protocol described in our previous paper [32] and as presented in Scheme 1. In the aforementioned study, we also conducted a comprehensive assessment of the chemical structure, molecular weight, as well as thermal, and crystalline properties. Summary of essential material's parameters are given in Table 1. Within the context of this research, we continued our investigation of the PDF-DLF material, with a particular emphasis on evaluating additional critical characteristics that are essential in determining the feasibility of utilizing furan-based copolymers in the biomedical sector.

https://doi.org/10.26434/chemrxiv-2023-0095d-v2 **ORCID:** https://orcid.org/0000-0002-2474-3517 Content not peer-reviewed by ChemRxiv. **License:** CC BY 4.0

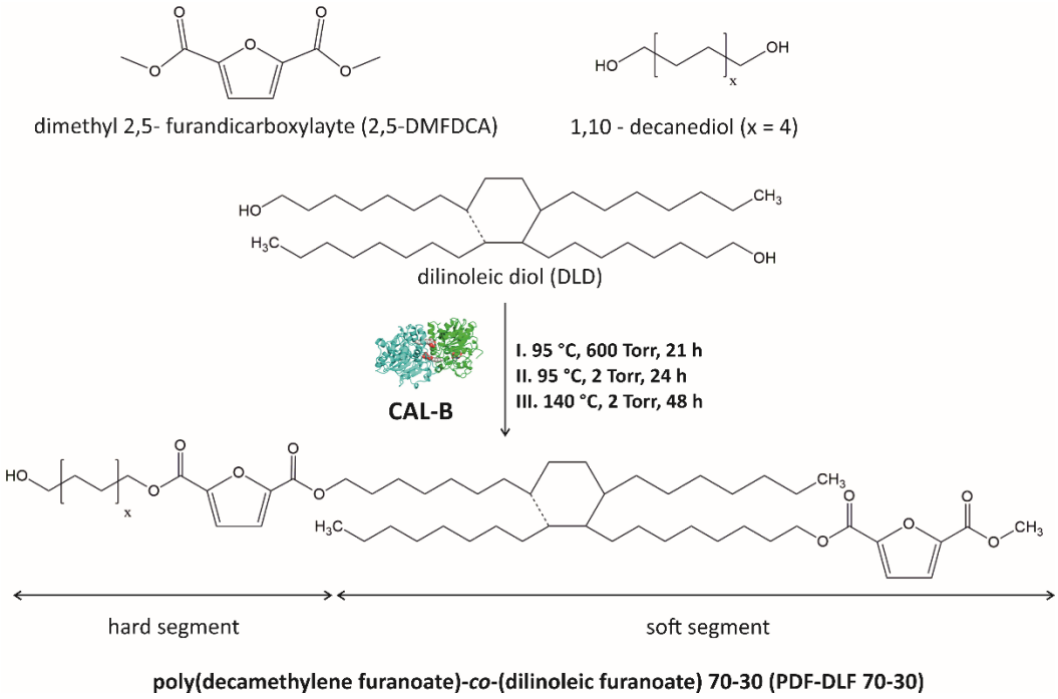

Scheme 1. General scheme of CAL-B catalyzed synthesis of poly(decamethylene furanoate)-co-(dilinoleic furanoate) copolyesters via the temperature-varied two-stage method in diphenyl ether. Adapted from [32].

Table 1. Physico-chemical characteristics of PDF-DLF copolyester.

^{1}H NMR[a]	DSC[a]					
Composition wt% [mol%]	**T_g [°C]**	**T_m [°C]**	**ΔH_m [J/g]**	**T_c [°C]**	**ΔH_c [J/g]**	**X_c [%]**
70.0-30.0 [84.0-16.0]	-20	95	34.40	27	30.77	17.4

T_g- glass transition temperature; ΔH_m- melting enthalpy of the hard segments; T_m- melting temperature; T_c-crystallization temperature; ΔH_c - crystallization enthalpy; X_c- total crystalline phase content in the polymer. DSC–Scanning Differential Calorimetry. [a]values provided from [32].

Dynamic Mechanical Thermal Analysis (DMTA) was performed to assess the mechanical properties of the PDF-DLF material (Fig. 1). The DMTA measurements indicate the viscoelastic characteristics of furan-based copolyesters, shedding light on their thermo-mechanical dynamics. Below the glass transition temperature (T_g), the copolyesters exhibited a consistently stable storage modulus. This stability indicates a solid and rigid nature within this temperature range, emphasizing the material's ability to maintain structural integrity and stiffness. Upon reaching the T_g, an evident decline in the storage modulus values became visible. This transition denotes a shift in molecular mobility, typically associated with a reduction in stiffness. The material undergoes a transformation toward increased flexibility, accompanied by heightened molecular movement, influencing its mechanical behavior. This particular aspect is

https://doi.org/10.26434/chemrxiv-2023-0095d-v2 **ORCID:** https://orcid.org/0000-0002-2474-3517 Content not peer-reviewed by ChemRxiv. **License:** CC BY 4.0

pertinent in applications where flexibility is a critical parameter. As the temperature continued to rise, the storage modulus gradually decreased until reaching the melting temperature (T_m). This gradual reduction in modulus values signifies a transition from a more solid to a more liquid-like state.

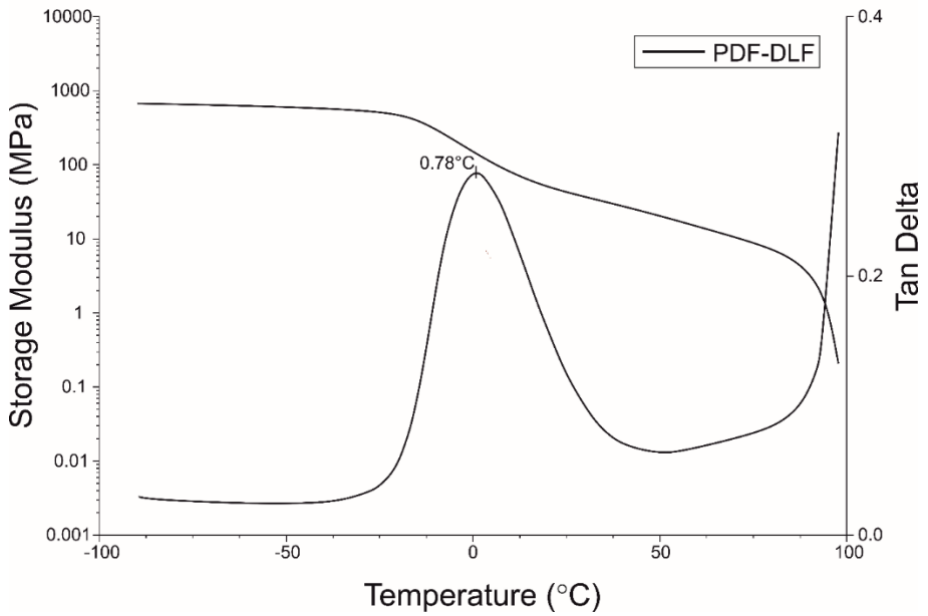

Figure 1. DMTA analysis of PDF-DLF copolyester.

Enzymatic degradation played a pivotal role in assessing the suitability of the PDF-DLF copolymer for biomedical applications. The material, subjected to lipase from *Pseudomonas cepacia* in a PBS solution, aimed to simulate physiological conditions within the human body. Understanding how the polymer undergoes enzymatic breakdown was essential for ensuring its compatibility with biological systems.

FTIR analysis before and after degradation revealed changes in intensities and shifts in peaks of characteristic functional groups (Fig. 2). A clear decrease in intensity is visible in the carbonyl group region (C=O), potentially indicating hydrolysis of ester bonds and monomer formation. This is further supported by the appearance of a peak arising from -OH groups. Additionally, changes are noted in the region where C=C bonds in the furan ring appear. These structural alterations suggest that the material undergoes disintegration under the influence of the enzyme.

https://doi.org/10.26434/chemrxiv-2023-0095d-v2 **ORCID:** https://orcid.org/0000-0002-2474-3517 Content not peer-reviewed by ChemRxiv. **License:** CC BY 4.0

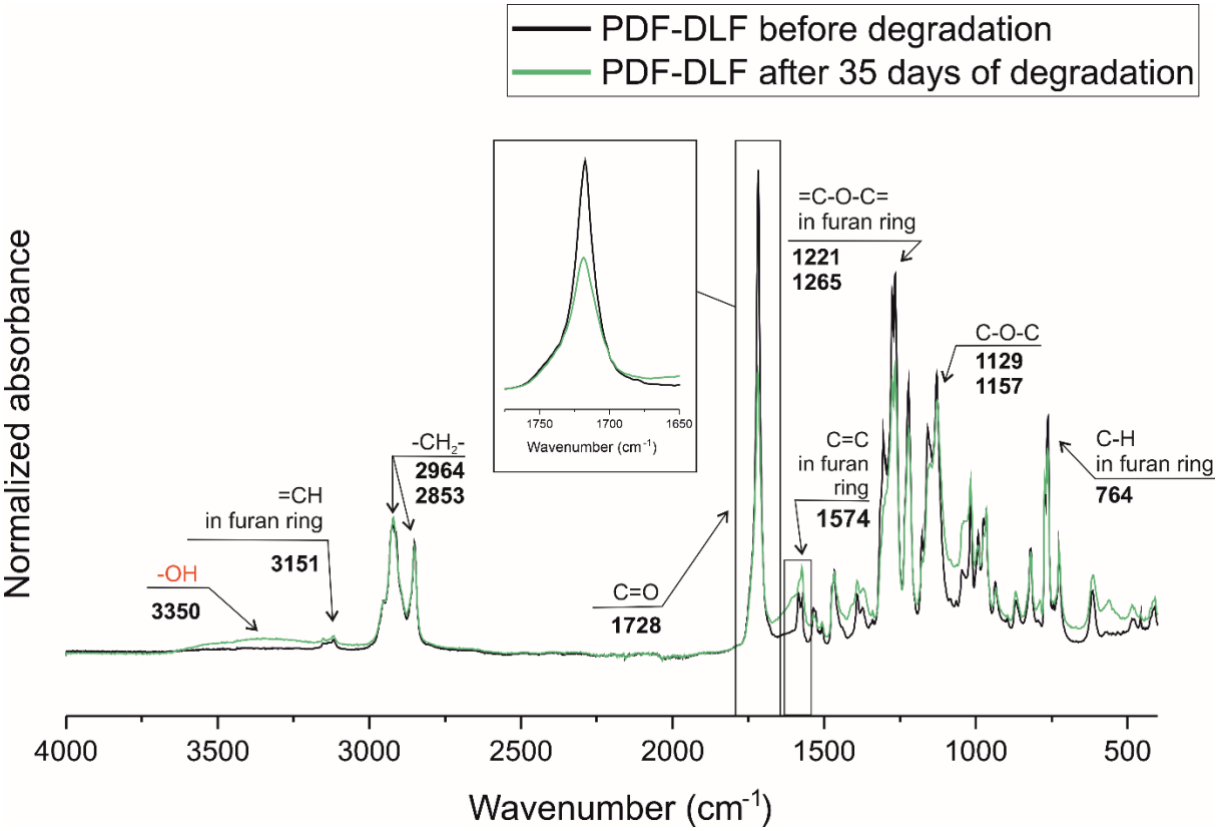

Figure 2. FTIR spectra of PDF-DLF copolymer before and after 35 days of enzymatic degradation.

Furthermore, to verify changes in the molecular weight, SEC measurements were conducted on materials both before and after 35 days of degradation. The observed molar mass changes (Table 2) along with the increased dispersity index suggest that the material has undergone enzymatic degradation. The degradation of polyesters with semi-aromatic structures is typically known to be relatively inefficient, however, in this case, it appears that the enzyme is targeting the amorphous regions, specifically the DLF soft segments. The visible alterations in molecular weight serve as a clear indicator of ester bond cleavage. This phenomenon is significant as it highlights the susceptibility of specific regions to enzymatic attack, contributing to the molecular rearrangement and changes observed.

Table 2. Molecular weight of PDF-DLF copolyester before and after degradation.

Material	**SEC**		
	M_n **[g/mol]**	M_w **[g/mol]**	$Đ$
PDF-DLF before degradation	12 200	43 600	3.6
PDF-DLF after 35 days of degradation	7 800	30 700	4.0

M_n – number average molecular mass, M_w – weight average molecular mass, $Đ$ – dispersity index.

https://doi.org/10.26434/chemrxiv-2023-0095d-v2 **ORCID:** https://orcid.org/0000-0002-2474-3517 Content not peer-reviewed by ChemRxiv. **License:** CC BY 4.0

Interestingly enough, SEM analysis displayed noticeable surface changes, including breaks and holes after degradation. Figure 3 illustrates these alterations on the material surface, indicating a localized impact. The results suggest that enzymatic degradation likely occurs through a surface erosion mechanism rather than extensive bulk breakdown.

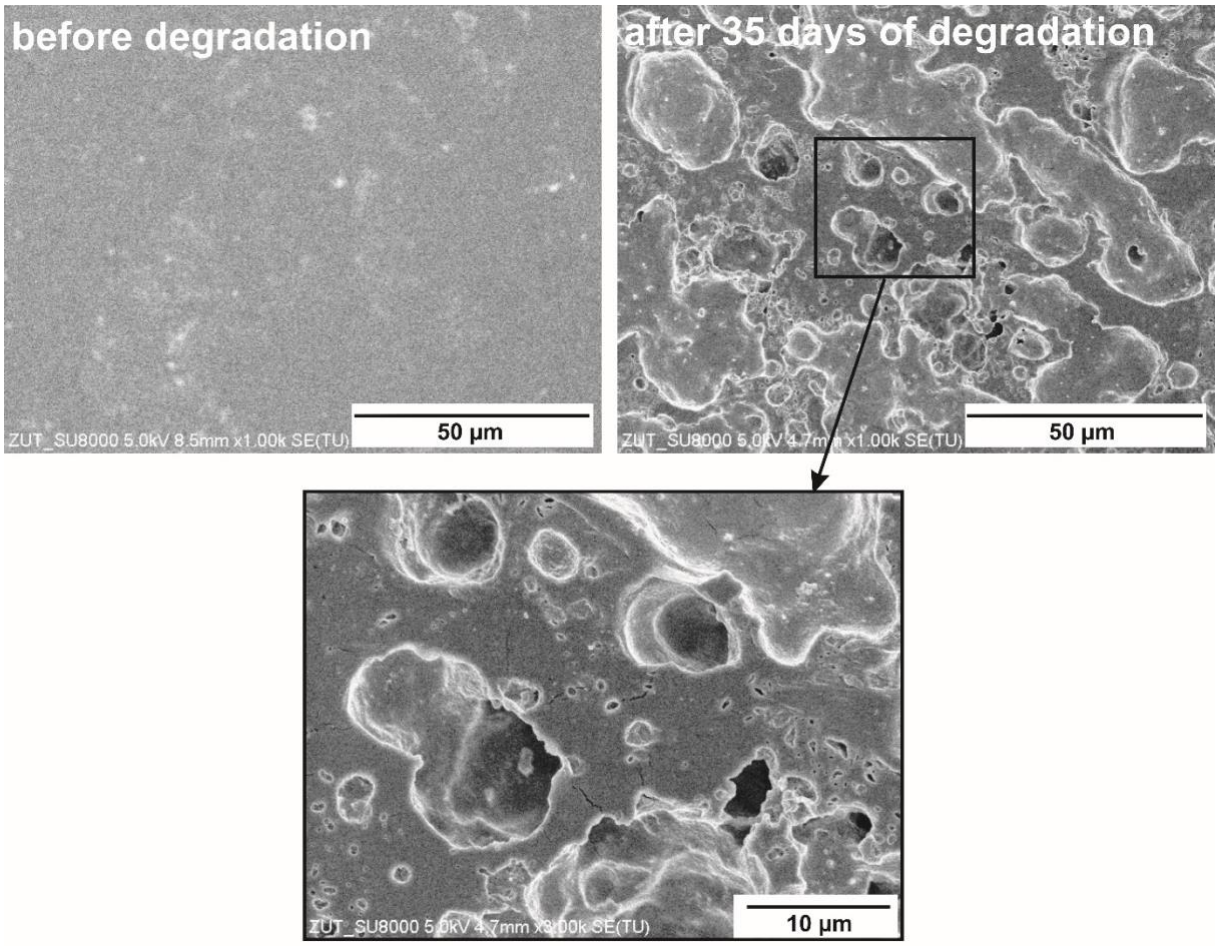

Figure 3. SEM images of PDF-DLF copolyester before and after 35 days of enzymatic degradation using lipase from *Pseudomonass cepacia*.

Finally, the detected mass loss of slightly more than 2% over 35 days indicated relatively slow progress of enzymatic degradation (Fig. 4). This behavior is typical of the first phase of enzyme-assisted chemical hydrolysis, and only after this is usually followed by metabolization of the fragments and rapid loss of polymer mass.

https://doi.org/10.26434/chemrxiv-2023-0095d-v2 **ORCID:** https://orcid.org/0000-0002-2474-3517 Content not peer-reviewed by ChemRxiv. **License:** CC BY 4.0

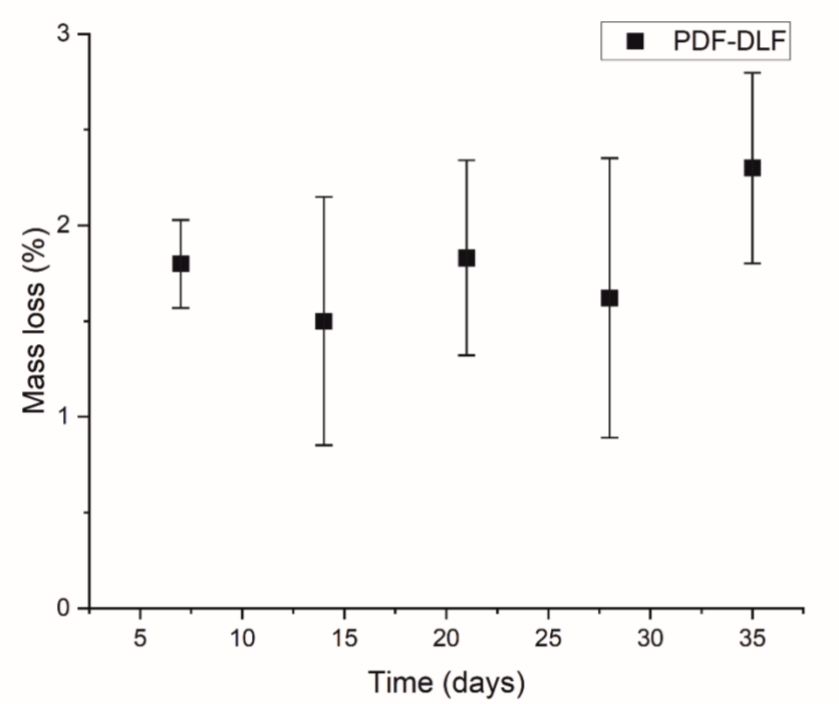

Figure 4. Mass loss of PDF-DLF copolyester during enzymatic degradation.

All these factors collectively suggest that PDF-DLF is susceptible to enzyme-assisted chemical hydrolysis, despite not significant mass loss. However, further in-depth investigation and research in this matter are necessary, potentially involving the use of different enzymes. For example, enzymatic degradation was also studied utilizing recombinant *Thermobifida cellulosilytica* cutinase *1* (Thc_Cut1), cutinase from *Humicola insolens* (HiC), and lipase from *Porcine pancreas* (LPP) on poly(ethylene furanoate) (PBF), revealing promising results and correlations [34–38]. Thc_Cut1 exhibited higher activity on higher molecular weight PEF powders, releasing 13 mM of FDCA after 72 hours [36]. Crystallinity significantly impacted degradation rates, accelerating hydrolysis in cases of lower crystallinity. On the other hand, HiC demonstrated greater activity than Thc_Cut1 on highly crystalline forms of PEF, thereby slowing enzymatic hydrolysis [34].

Moreover, a recent study by Kim *et al.* explored the enzymatic degradation of poly(butylene adipate)-co-(butylene furanoate) (PBAF) copolymers with varying furan ring fractions (50 and 70 mol%) using *Thermomyces lanuginosus* lipase (TLL), a highly selective catalyst [39]. The study revealed that PBAF with a 50 mol% furan ring fraction experienced a mass loss exceeding 80% within a few days, while PBAF with a 70 mol% furan ring fraction exhibited only around 1-2% mass loss over the same period. These findings align with our research, indicating that a higher proportion of furan units in the copolymer results in a slower rate of degradation. Hence, careful design considerations for such materials are essential to accelerate this process, particularly for meeting the requirements of medical applications. All enzymes used

https://doi.org/10.26434/chemrxiv-2023-0095d-v2 **ORCID:** https://orcid.org/0000-0002-2474-3517 Content not peer-reviewed by ChemRxiv. **License:** CC BY 4.0

for the enzymatic degradation studies acknowledged above were in their native form (not immobilized).

Given the potential application of the copolymer in the biomedical field, specifically in contact with the body, it became imperative to assess the material's biocompatibility. To investigate any potential cytotoxic or growth-inhibitory effects of the PDF-DLF copolyester, an *in vitro* indirect contact assay was conducted using L929 murine fibroblasts. Over 24 hours, cells were exposed to extracts from both the reference material (PCL) and the PDF-DLF samples, and viability was assessed through an inverted light microscope and the resazurin viability assay. Following the 24-hour incubation, noticeable adverse effects of both PCL and PDF-DLF materials were observed, as illustrated in Figure 5. Importantly, the absence of toxic contaminants was confirmed by the robust growth and typical cell morphology observed in extracts from control, reference, and tested materials. The microscopic observations were supported by the results of the resazurin viability assay, from which normalized viability values were calculated. These values were in accordance with the visual evaluation. Considering the typical doubling time of L929 cells is approximately 20-22 hours, viability values below 70% are indicative of cytotoxicity according ISO10993. The average values of normalized cells viability (CV%) for PCL and PDF-DLF were 97 ± 5 and 95 ± 7%, respectively.

https://doi.org/10.26434/chemrxiv-2023-0095d-v2 **ORCID:** https://orcid.org/0000-0002-2474-3517 Content not peer-reviewed by ChemRxiv. **License:** CC BY 4.0

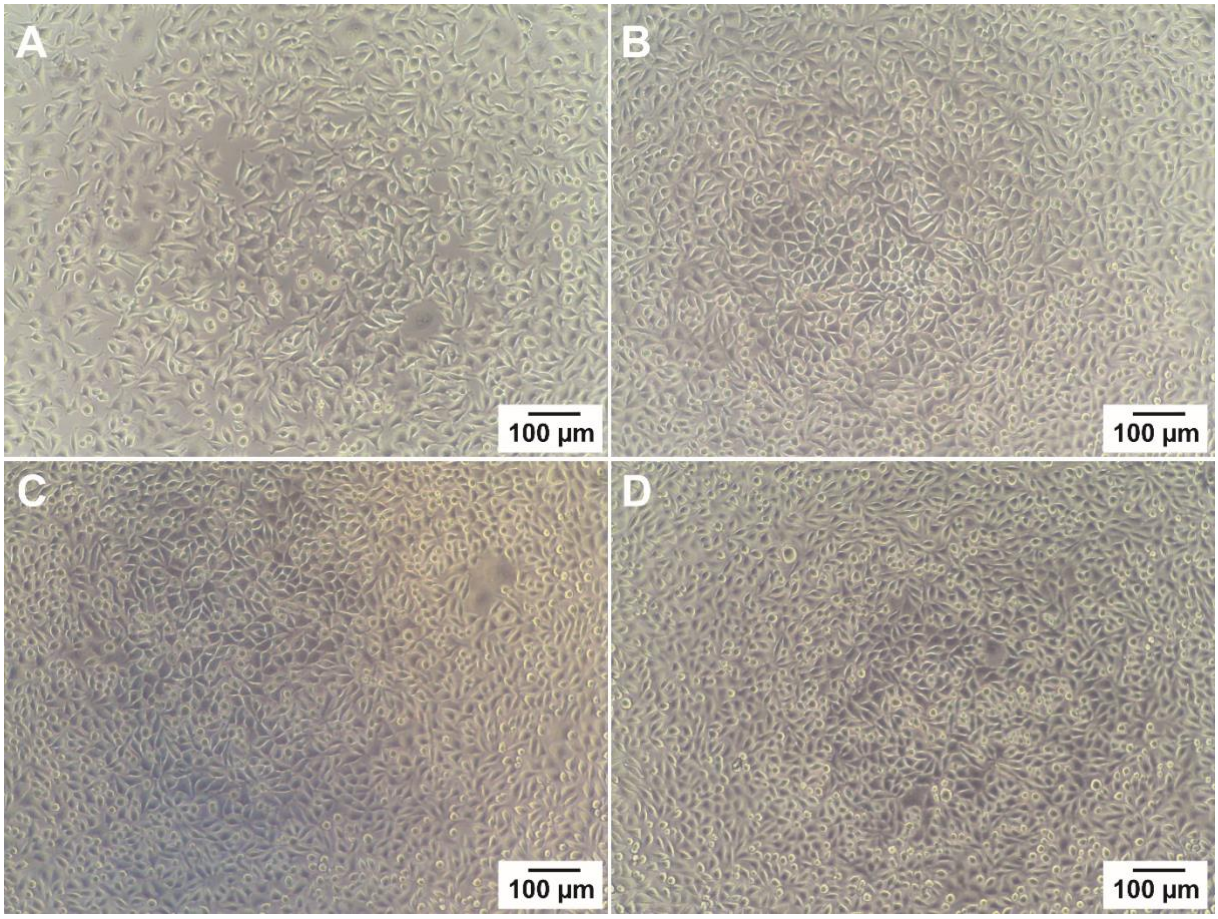

Figure 5. Representative micrographs of L929 cells seeded at 10000 cells per well. A) Cells 24 hours after seeding. B) Cells 48 hours of culture without extracts. Cells were cultured for 24 hours with extracts from C) tested PDF-DLF material and D) reference material (PCL sample).

Ultimately, PDF-DLF underwent a preliminary study involving electrospinning to assess its processability and suitability for application in the field of tissue engineering as scaffolds.

In the course of our investigations, it was observed that polymer concentrations below 20% resulted in electro-spraying, revealing inadequate fiber formation, while a concentration of 50% led to the formation of a bulk structure. This was attributed to the solvent evaporation rate on crystalline phase formation of the polymer during electrospinning, which can be irrespective of polymer drawing forces [40].

Subsequent experimental studies identified that the optimum polymer concentration of 30%, coupled with a 24-gauge needle, yielded the most favorable electrospinning outcomes. The fine-tuning process extended beyond concentration adjustment and encompassed modifications to key electrospinning parameters, including the distance between the needle tip and the collector, applied voltage, and polymer solution flow rate. Through systematic adjustments, the following optimal

https://doi.org/10.26434/chemrxiv-2023-0095d-v2 **ORCID:** https://orcid.org/0000-0002-2474-3517 Content not peer-reviewed by ChemRxiv. **License:** CC BY 4.0

parameters were identified: a distance of 20 cm, a flow rate of 5 mL/h, and an applied voltage of 15 kV. The establishment of these conditions not only enabled the reproducibility of the electrospinning process but also underscored the importance of optimal parameters in governing the morphological characteristics of the resulting fibers.

Figure 6 represents the SEM images of the obtained fibers through the optimized parameters of the electrospinning. It is evident that the acquired fibers exhibit structural homogeneity and uniform distribution. Given the utilization of a flat aluminum collector during the electrospinning process, the resultant fibers exhibit a random orientation. Figure 7 presents a comprehensive analysis of fiber diameters and their distribution, conducted through Image J software. The findings reveal that, for the copolymer under investigation, the majority of fiber diameters fall within the range of 500-700 nm. This outcome underscores the electrospinning potential of the polymer, showcasing characteristics similar to the native extracellular matrix (ECM) [41,42]. The versatility of these fibers extends their applicability to diverse domains, including, but not only limited to tissue engineering.

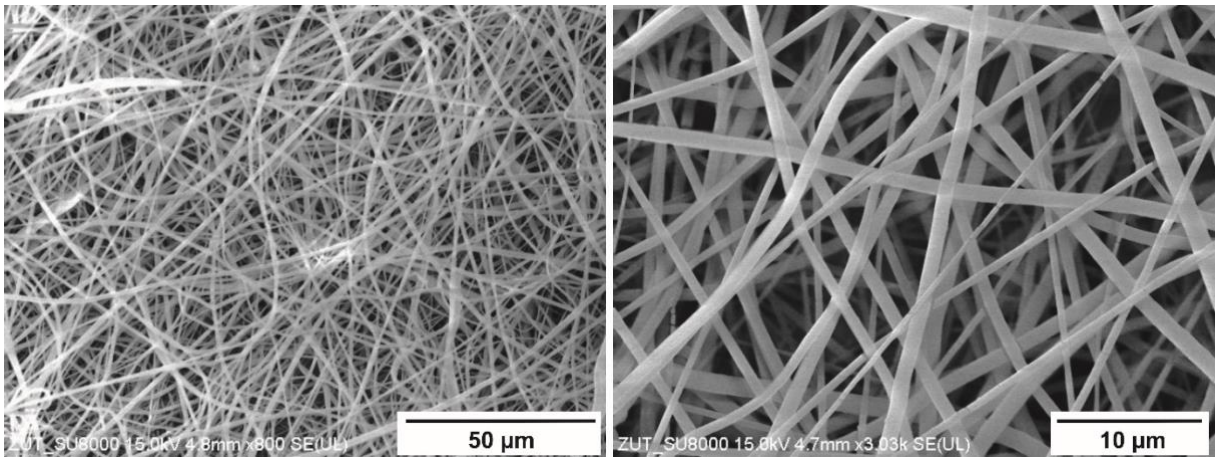

Figure 6. SEM micrographs of the obtained fibers from PDF-DLF copolymer using $CHCl_3$ as the solvent with 30% wt/vol% concentration.

https://doi.org/10.26434/chemrxiv-2023-0095d-v2 **ORCID:** https://orcid.org/0000-0002-2474-3517 Content not peer-reviewed by ChemRxiv. **License:** CC BY 4.0

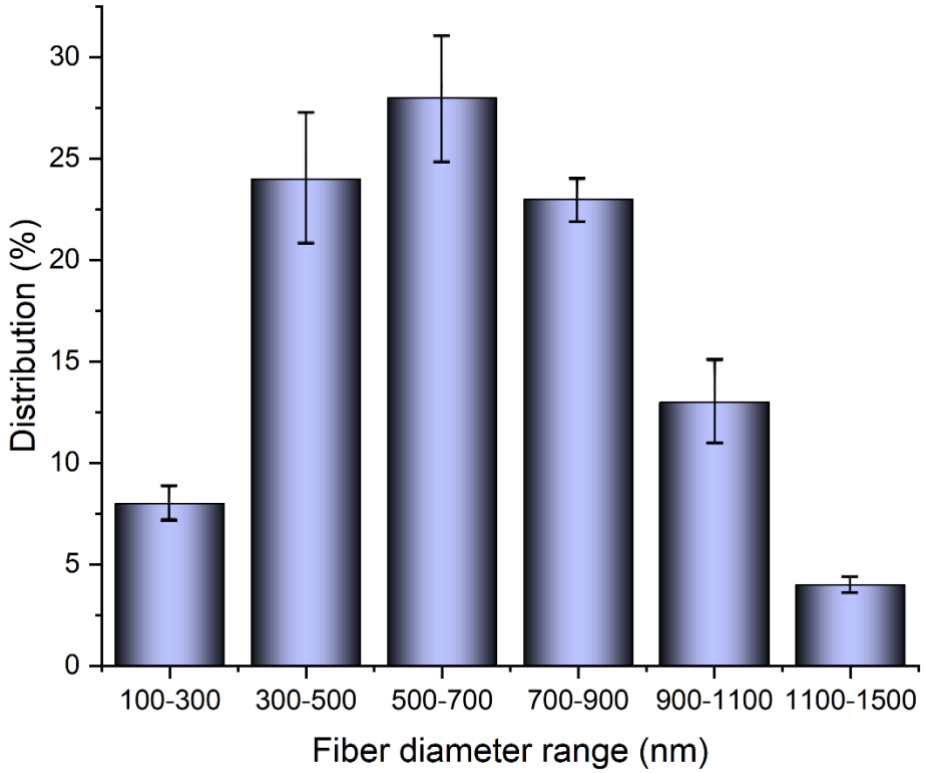

Figure 7. Fiber diameter distribution obtained from SEM micrographs of the copolymer, using Image J software.

3 Conclusions

In response to the increasing demand for sustainable materials, particularly in the polyester domain, this research has been dedicated to the comprehensive evaluation of a furan-based copolymer, poly(decamethylene furanoate)-co-(dilinoleic furanoate) (PDF-DLF). The copolymer, with a 70-30 wt% hard-to-soft segment ratio, was examined for its potential in medical applications, with a specific emphasis on its viability as scaffolding material for tissue engineering.

The results underscore the significant steps made in the development of sustainable materials with versatile processing capabilities. PDF-DLF exhibited promising mechanical and thermal properties. Its successful electrospinning into nanofibers, with diameters ranging from 500 to 700 nm, holds promise for the creation of biodegradable scaffolds for medical engineering.

Furthermore, the biocompatibility assessments revealed promising results. *In vitro* studies using L929 murine fibroblasts demonstrated high cell viability, indicating the material's compatibility and lack of cytotoxic effects. Enzymatic degradation studies, though indicating relatively slow progress, revealed structural changes, molecular mass changes, and localized impacts on the material's surface, suggesting susceptibility to enzymatic breakdown. However, while this study has unveiled promising aspects of PDF-DLF, further research is imperative. Deeper research on

https://doi.org/10.26434/chemrxiv-2023-0095d-v2 **ORCID:** https://orcid.org/0000-0002-2474-3517 Content not peer-reviewed by ChemRxiv. **License:** CC BY 4.0

enzymatic degradation mechanisms, which could utilize different enzymes, is recommended.

In conclusion, the findings of this research not only contribute to the expanding knowledge on sustainable materials but also open new avenues for PDF-DLF in critical industries, particularly in the ever-evolving field of biomedical engineering. The convergence of biocompatibility, mechanical properties, and processing capabilities in PDF-DLF suggests a multifaceted solution to environmental and engineering challenges, warranting continued exploration and refinement.

Abbreviations

Đ, dispersity index; CAL-B, *Candida antarctica* lipase type B; $CDCl_3$, deuterated chloroform; DDO, 1,10 – decanediol; DE, diphenyl ether; DLD, dilinoleic diol; DPBS, Dulbecco's Phosphate Buffered Saline; DMEM, Dulbecco's Modified Eagle's Medium; DMFDCA, dimethyl 2,5-furandicarboxylate; DMTA, dynamic thermos-mechanical analysis; DPBS, Dulbecco's Phosphate Buffered Saline; DSC, differential scanning calorimetry; ECM, extracellular matrix; FBS, fetal bovine serum; FTIR, Fourier Transform Infrared Spectroscopy; FDCA, 2,5 – furandicarboxylic acid; HiC, cutinase from *Humicola insolens*; LPP, lipase from *Porcine pancreas*; M_n, number averaged molecular weight; M_w, weight averaged molecular weight; PET, poly(ethylene terephthalate); PBAF, poly(butylene adipate)-co-(butylene furanoate); PBF, poly(butylene furanoate); PCL, polycaprolactone; PET, poly(ethylene terephthalate); PDF-DLF, poly(decamethylene furanoate)-*co*-(dilinoleic furanoate); SEC, size exclusion chromatography; SEM, scanning electron microscope; Thc_Cut1, *Thermobifida cellulosilytica* cutinase *1*; TLL, *Thermomyces lanuginosus* lipase; T_c, crystallization temperature; T_g, glass transition temperature; T_m, melting temperature; TPA, terephthalic acid; ΔH_m, melting enthalpy; $\Delta H_m°$, melting enthalpy of fully crystalline polyester; ΔH_c, crystallization enthalpy.

Author Contributions

Martyna Sokołowska was responsible for methodology, investigation, validation, formal analysis, writing (original draft), and visualization. **Moein Zarei** was responsible for the electrospinning process methodology, optimization, and investigation. **Miroslawa El Fray** was responsible for conceptualization, supervision, writing (review & editing), project administration, and fund raising.

Conflicts of interest

The authors declare that there are no conflicts to declare.

https://doi.org/10.26434/chemrxiv-2023-0095d-v2 **ORCID:** https://orcid.org/0000-0002-2474-3517 Content not peer-reviewed by ChemRxiv. **License:** CC BY 4.0

Acknowledgments

This work has received funding from the European Union's Horizon 2020 research and innovation program under the Marie Skłodowska-Curie grant agreement no. 872152 (GREEN MAP). An international project co-financed by the program of the Minister of Science and Higher Education entitled "PMW" in the years 2000-2023; contract No. 5091/H2020/2020/2 is acknowledged.

References

[1] Eerhart AJJE, Faaij APC, Patel MK. Replacing fossil based PET with biobased PEF; process analysis, energy and GHG balance. Energy Environ Sci 2012;5:6407. https://doi.org/10.1039/c2ee02480b.

[2] Abdolmohammadi S, Gansebom D, Goyal S, Lee T-H, Kuehl B, Forrester MJ, et al. Analysis of the Amorphous and Interphase Influence of Comononomer Loading on Polymer Properties toward Forwarding Bioadvantaged Copolyamides. Macromolecules 2021;54:7910–24. https://doi.org/10.1021/acs.macromol.1c00651.

[3] Sousa AF, Vilela C, Fonseca AC, Matos M, Freire CSR, Gruter G-JM, et al. Biobased polyesters and other polymers from 2,5-furandicarboxylic acid: a tribute to furan excellency. Polym Chem 2015;6:5961–83. https://doi.org/10.1039/C5PY00686D.

[4] Esteban J, Yustos P, Ladero M. Catalytic Processes from Biomass-Derived Hexoses and Pentoses: A Recent Literature Overview. Catalysts 2018;8:637. https://doi.org/10.3390/catal8120637.

[5] Kwiatkowska M, Kowalczyk I, Kwiatkowski K, Szymczyk A, Rosłaniec Z. Fully biobased multiblock copolymers of furan-aromatic polyester and dimerized fatty acid: Synthesis and characterization. Polymer (Guildf) 2016;99:503–12. https://doi.org/10.1016/j.polymer.2016.07.060.

[6] Bozell JJ, Petersen GR. Technology development for the production of biobased products from biorefinery carbohydrates—the US Department of Energy's "Top 10" revisited. Green Chemistry 2010;12:539. https://doi.org/10.1039/b922014c.

[7] Zhu J, Cai J, Xie W, Chen P-H, Gazzano M, Scandola M, et al. Poly(butylene 2,5-furan dicarboxylate), a Biobased Alternative to PBT: Synthesis, Physical Properties, and Crystal Structure. Macromolecules 2013;46:796–804. https://doi.org/10.1021/ma3023298.

https://doi.org/10.26434/chemrxiv-2023-0095d-v2 **ORCID:** https://orcid.org/0000-0002-2474-3517 Content not peer-reviewed by ChemRxiv. **License:** CC BY 4.0

[8] Zhou W, Zhang Y, Xu Y, Wang P, Gao L, Zhang W, et al. Synthesis and characterization of bio-based poly(butylene furandicarboxylate)-b-poly(tetramethylene glycol) copolymers. Polym Degrad Stab 2014;109:21–6. https://doi.org/10.1016/j.polymdegradstab.2014.06.018.

[9] Ma J, Pang Y, Wang M, Xu J, Ma H, Nie X. The copolymerization reactivity of diols with 2,5-furandicarboxylic acid for furan-based copolyester materials. J Mater Chem 2012;22:3457. https://doi.org/10.1039/c2jm15457a.

[10] Bianchi E, Soccio M, Siracusa V, Gazzano M, Thiyagarajan S, Lotti N. Poly(butylene 2,4-furanoate), an Added Member to the Class of Smart Furan-Based Polyesters for Sustainable Packaging: Structural Isomerism as a Key to Tune the Final Properties. ACS Sustain Chem Eng 2021;9:11937–49. https://doi.org/10.1021/acssuschemeng.1c04104.

[11] Papageorgiou GZ, Papageorgiou DG, Tsanaktsis V, Bikiaris DN. Synthesis of the bio-based polyester poly(propylene 2,5-furan dicarboxylate). Comparison of thermal behavior and solid state structure with its terephthalate and naphthalate homologues. Polymer (Guildf) 2015;62:28–38. https://doi.org/10.1016/j.polymer.2015.01.080.

[12] Jiang M, Liu Q, Zhang Q, Ye C, Zhou G. A series of furan-aromatic polyesters synthesized via direct esterification method based on renewable resources. J Polym Sci A Polym Chem 2012;50:1026–36. https://doi.org/10.1002/pola.25859.

[13] Manuel HJ, Gaymans RJ. Segmented block copolymers based on poly(butylene terephthalate) and telechelic polyesters and polyamides of dimerized fatty acids. Polymer (Guildf) 1993;34:4325–9. https://doi.org/10.1016/0032-3861(93)90196-H.

[14] Mathers RT. How well can renewable resources mimic commodity monomers and polymers? J Polym Sci A Polym Chem 2012;50:1–15. https://doi.org/10.1002/pola.24939.

[15] Jiang Y, Woortman AJJ, Alberda van Ekenstein GOR, Loos K. Enzyme-catalyzed synthesis of unsaturated aliphatic polyesters based on green monomers from renewable resources. Biomolecules 2013;3:461–80. https://doi.org/10.3390/biom3030461.

[16] Jiang Y, Woortman AJJ, Alberda Van Ekenstein GOR, Loos K. Environmentally benign synthesis of saturated and unsaturated aliphatic polyesters via enzymatic polymerization of biobased monomers derived from renewable resources. Polym Chem 2015;6:5451–63. https://doi.org/10.1039/c5py00660k.

https://doi.org/10.26434/chemrxiv-2023-0095d-v2 **ORCID:** https://orcid.org/0000-0002-2474-3517 Content not peer-reviewed by ChemRxiv. **License:** CC BY 4.0

[17] Jiang Y, Loos K. Enzymatic Synthesis of Biobased Polyesters and Polyamides. Polymers (Basel) 2016;8:243. https://doi.org/10.3390/polym8070243.

[18] Fei X, Wang J, Zhu J, Wang X, Liu X. Biobased Poly(ethylene 2,5-furancoate): No Longer an Alternative, but an Irreplaceable Polyester in the Polymer Industry. ACS Sustain Chem Eng 2020;8:8471–85. https://doi.org/10.1021/acssuschemeng.0c01862.

[19] Jiang Y, Woortman AJJ, Alberda van Ekenstein GOR, Petrović DM, Loos K. Enzymatic Synthesis of Biobased Polyesters Using 2,5-Bis(hydroxymethyl)furan as the Building Block. Biomacromolecules 2014;15:2482–93. https://doi.org/10.1021/bm500340w.

[20] Douka A, Vouyiouka S, Papaspyridi LM, Papaspyrides CD. A review on enzymatic polymerization to produce polycondensation polymers: The case of aliphatic polyesters, polyamides and polyesteramides. Prog Polym Sci 2018;79:1–25. https://doi.org/10.1016/j.progpolymsci.2017.10.001.

[21] Puskas JE, Sen MY, Seo KS. Green polymer chemistry using nature's catalysts, enzymes. J Polym Sci A Polym Chem 2009;47:2959–76. https://doi.org/10.1002/pola.23351.

[22] KOBAYASHI S. Lipase-catalyzed polyester synthesis - A green polymer chemistry. Proceedings of the Japan Academy, Series B 2010;86:338–65. https://doi.org/10.2183/pjab.86.338.

[23] Kobayashi S. Enzymatic polymerization: A new method of polymer synthesis. J Polym Sci A Polym Chem 1999;37:3041–56. https://doi.org/10.1002/(SICI)1099-0518(19990815)37:16<3041::AID-POLA1>3.0.CO;2-V.

[24] Kobayashi S, Uyama H, Kimura S. Enzymatic Polymerization. Chem Rev 2001;101:3793–818. https://doi.org/10.1021/cr9901211.

[25] Sokołowska M, Nowak-Grzebyta J, Stachowska E, El Fray M. Enzymatic Catalysis in Favor of Blocky Structure and Higher Crystallinity of Poly(Butylene Succinate)-Co-(Dilinoleic Succinate) (PBS-DLS) Copolymers of Variable Segmental Composition. Materials 2022;15:1132. https://doi.org/10.3390/ma15031132.

[26] Sokołowska M, Stachowska E, Czaplicka M, El Fray M. Effect of enzymatic versus titanium dioxide/silicon dioxide catalyst on crystal structure of 'green'

https://doi.org/10.26434/chemrxiv-2023-0095d-v2 **ORCID:** https://orcid.org/0000-0002-2474-3517 Content not peer-reviewed by ChemRxiv. **License:** CC BY 4.0

poly[(butylene succinate)- co -(dilinoleic succinate)] copolymers. Polym Int 2021;70:514–26. https://doi.org/10.1002/pi.6104.

[27] Skoczinski P, Espinoza Cangahuala MK, Maniar D, Albach RW, Bittner N, Loos K. Biocatalytic Synthesis of Furan-Based Oligomer Diols with Enhanced End-Group Fidelity. ACS Sustain Chem Eng 2020;8:1068–86. https://doi.org/10.1021/acssuschemeng.9b05874.

[28] Tsujimoto T, Uyama H, Kobayashi S. Enzymatic Synthesis of Cross-Linkable Polyesters from Renewable Resources. Biomacromolecules 2001;2:29–31. https://doi.org/10.1021/bm000097h.

[29] Japu C, Martínez de Ilarduya A, Alla A, Jiang Y, Loos K, Muñoz-Guerra S. Copolyesters Made from 1,4-Butanediol, Sebacic Acid, and Glucose by Melt and Enzymatic Polycondensation. Biomacromolecules 2015;16:868–79. https://doi.org/10.1021/bm501771e.

[30] Juais D, Naves AF, Li C, Gross RA, Catalani LH. Isosorbide Polyesters from Enzymatic Catalysis. Macromolecules 2010;43:10315–9. https://doi.org/10.1021/ma1013176.

[31] Dong Y, Liao S, Ngiam M, Chan CK, Ramakrishna S. Degradation Behaviors of Electrospun Resorbable Polyester Nanofibers. Tissue Eng Part B Rev 2009;15:333–51. https://doi.org/10.1089/ten.teb.2008.0619.

[32] Sokołowska M, Nowak-Grzebyta J, Stachowska E, Miądlicki P, Zdanowicz M, Michalkiewicz B, et al. Enzymatically catalyzed furan-based copolyesters containing dilinoleic diol as a building block. RSC Adv 2023;13:22234–49. https://doi.org/10.1039/D3RA03885H.

[33] Ciecholewska-Juśko D, Żywicka A, Junka A, Drozd R, Sobolewski P, Migdał P, et al. Superabsorbent crosslinked bacterial cellulose biomaterials for chronic wound dressings. Carbohydr Polym 2021;253:117247. https://doi.org/10.1016/j.carbpol.2020.117247.

[34] Weinberger S, Haernvall K, Scaini D, Ghazaryan G, Zumstein MT, Sander M, et al. Enzymatic surface hydrolysis of poly(ethylene furanoate) thin films of various crystallinities. Green Chemistry 2017;19:5381–4. https://doi.org/10.1039/C7GC02905E.

https://doi.org/10.26434/chemrxiv-2023-0095d-v2 **ORCID:** https://orcid.org/0000-0002-2474-3517 Content not peer-reviewed by ChemRxiv. **License:** CC BY 4.0

[35] Weinberger S, Canadell J, Quartinello F, Yeniad B, Arias A, Pellis A, et al. Enzymatic Degradation of Poly(ethylene 2,5-furanoate) Powders and Amorphous Films. Catalysts 2017;7:318. https://doi.org/10.3390/catal7110318.

[36] Pellis A, Haernvall K, Pichler CM, Ghazaryan G, Breinbauer R, Guebitz GM. Enzymatic hydrolysis of poly(ethylene furanoate). J Biotechnol 2016;235:47–53. https://doi.org/10.1016/j.jbiotec.2016.02.006.

[37] Gigli M, Quartinello F, Soccio M, Pellis A, Lotti N, Guebitz GM, et al. Enzymatic hydrolysis of poly(1,4-butylene 2,5-thiophenedicarboxylate) (PBTF) and poly(1,4-butylene 2,5-furandicarboxylate) (PBF) films: A comparison of mechanisms. Environ Int 2019;130:104852. https://doi.org/10.1016/j.envint.2019.05.046.

[38] Lalanne L, Nyanhongo GS, Guebitz GM, Pellis A. Biotechnological production and high potential of furan-based renewable monomers and polymers. Biotechnol Adv 2021;48:107707. https://doi.org/10.1016/j.biotechadv.2021.107707.

[39] Kim H, Kim T, Choi S, Jeon H, Oh DX, Park J, et al. Remarkable elasticity and enzymatic degradation of bio-based poly(butylene adipate- *co* -furanoate): replacing terephthalate. Green Chemistry 2020;22:7778–87. https://doi.org/10.1039/D0GC01688H.

[40] Costa LMM, Bretas RES, Gregorio R. Effect of Solution Concentration on the Electrospray/Electrospinning Transition and on the Crystalline Phase of PVDF. Materials Sciences and Applications 2010;01:247–52. https://doi.org/10.4236/msa.2010.14036.

[41] Zarei M, Żwir MJ, Wiśniewska E, Michalkiewicz B, El Fray M. Melt and solution processability of poly(butylene succinate-dilinoleic succinate) copolymers modified with poly(ethylene glycol) using <scp>3D</scp> printing and electrospinning. Polym Adv Technol 2023;34:3586–602. https://doi.org/10.1002/pat.6159.

[42] Wei Q, Tao D, Xu Y. Nanofibers: principles and manufacture. Functional Nanofibers and their Applications, Elsevier; 2012, p. 3–21. https://doi.org/10.1533/9780857095640.1.1.

https://doi.org/10.26434/chemrxiv-2023-0095d-v2 **ORCID:** https://orcid.org/0000-0002-2474-3517 Content not peer-reviewed by ChemRxiv. **License:** CC BY 4.0